Altered hepatic sphingolipid metabolism in insulin resistant mice

Free Radical Biology and Medicine 169 (2021) 425–435

Contents lists available at ScienceDirect

Free Radical Biology and Medicine

journal homepage: www.elsevier.com/locate/freeradbiomed

Original article

Altered hepatic sphingolipid metabolism in insulin resistant mice: Role of advanced glycation endproducts

Raffaella Mastrocola [a,b,*], Federica Dal Bello [c], Alessia S. Cento [a], Katrien Gaens [b], Debora Collotta [d], Manuela Aragno [a], Claudio Medana [c], Massimo Collino [d], Kristiaan Wouters [b], Casper G. Schalkwijk [b]

[a] Dept. of Clinical and Biological Sciences, University of Turin, Italy
[b] Dept. of Internal Medicine, MUMC+, Maastricht, Limburg, Cardiovascular Research Institute, Maastricht (CARIM), the Netherlands
[c] Dept. of Molecular Biotechnology and Health Sciences, University of Turin, Italy
[d] Dept. of Drug Science and Technology, University of Turin, Italy

ARTICLE INFO

Keywords:
Sphngosine-1-Phosphate
Ceramide
Pyridoxamine
Advanced glycation end-products
Carboxymethyllysine
Insulin resistance

ABSTRACT

High plasma levels of the sphingolipid intermediates ceramide (Cer) and sphingosine-1-phosphate (S1P) are suggested to be involved in the development of insulin resistance (IR). Recent evidence indicates that advanced glycation endproducts (AGEs) can alter the sphingolipids metabolism equilibrium. Since enzymes responsible for sphingolipid rheostat maintenance are highly expressed in liver, we thus investigated whether AGEs accumulation can affect hepatic sphingolipids metabolism in insulin resistant mice.

Two different models of IR were examined: genetically diabetic LeptrDb-/- (DbDb) and diet-induced insulin resistant C57Bl/6J mice fed a 60% *trans*-fat diet (HFD). In addition, a group of HFD mice was supplemented with the anti-AGEs compound pyridoxamine. AGEs were evaluated in the liver by western blotting. Cer and S1P were measured by UHPLC-MS/MS. The expression of RAGE and of enzymes involved in sphingolipid metabolism were assessed by RT-PCR and western blotting. HepG2 cells were used to study the effect of the major AGE Nε-(carboxymethyl)lysine (CML)-albumin on sphingolipid metabolism and the role of the receptor of AGEs (RAGE).

High levels of AGEs and RAGE were detected in the liver of both DbDb and HFD mice in comparison to controls. The expression of enzymes of sphingolipid metabolism was altered in both models, accompanied by increased levels of Cer and S1P. Specifically, ceramide synthase 5 and sphingosine kinase 1 were increased, while neutral ceramidase was reduced. Pyridoxamine supplementation to HFD mice diminished hepatic AGEs and prevented alterations of sphingolipid metabolism and the development of IR. CML administration to HepG2 cells evoked alterations similar to those observed *in vivo*, that were in part mediated by the binding to RAGE.

The present study shows a direct involvement of AGEs in alterations of sphingolipid metabolism associated to the development of IR. The modulation of sphingolipids metabolism through the prevention of AGEs accumulation by pyridoxamine may reduce the development of IR.

1. Introduction

Obesity, specifically when implying visceral fat accumulation, is a common feature of the metabolic syndrome and often represents a central player for the concomitant development of insulin resistance (IR). Indeed, diet-induced obesity is accompanied by modifications of lipid metabolism with altered composition in lipid intermediates that exert detrimental effects in several organs [1]. In particular, the levels of the sphingolipid intermediates ceramide (Cer), sphingosine (Sph) and sphingosine-1-phosphate (S1P) have been reported to be unbalanced in metabolic diseases [2]. Under physiological conditions, Cer/Sph/S1P concentrations are tightly regulated by the activity of coordinated enzymes and maintained in a kind of equilibrium, the so called "sphingolipids rheostat", in which Sph represents the centre of a balance with Cer and S1P at the opposite extremes [3]. Cer and S1P levels are found to be increased in the plasma of obese and diabetic patients [4–6]. It has been demonstrated that the disturbance of the Cer/Sph/S1P equilibrium exerts a key role in inflammatory response and IR onset [7,8]. The enzymes regulating the sphingolipids metabolism are largely expressed in

* Corresponding author. Department of Clinical and Biological Sciences, Corso Raffaello 30, 10125, Turin, Italy.
E-mail address: raffaella.mastrocola@unito.it (R. Mastrocola).

https://doi.org/10.1016/j.freeradbiomed.2021.04.028
Received 9 February 2021; Received in revised form 15 April 2021; Accepted 20 April 2021
Available online 24 April 2021

Abbreviations

ACC	acetyl coenzyme A carboxylase
AGEs	Advanced glycation endproducts
Akt	alpha serine/threonine-protein kinase; Cer, ceramide;
CerS5	ceramide synthase 5
CML,	carboxymethyllysine;
FASN	fatty acid synthase
GSK-3β	glycogen synthase kinase 3 beta
IR	insulin resistance
IRS1	insulin receptor substrate 1
MG	methylglyoxal; nCdase, neutral ceramidase
RAGE	receptor for AGEs
S1P	sphingosine-1-phosphate
S1PR1-5	sphingosine-1-phosphate receptors 1–5
SCAP	SREBP cleavage activating protein
Sph	sphingosine;
SphK1	sphingosine kinase 1
SphK2	sphingosine kinase 2
SREBP1c	sterol regulatory element binding protein-1c

the gastrointestinal system with the highest levels in the liver [9], were Cer and S1P have been involved in the development of NASH and hepatic insulin resistance [10].

In this context, some studies have demonstrated that the inhibition of Cer synthesis prevents lipid-induced IR, diet-induced IR, and hepatic steatosis [11,12]. Moreover, S1P either acts inside the cell as a second messenger in several pathways or can be secreted out of the cell and exert a paracrine action through the binding to five specific receptors (S1PR1-5) [2,8], some of which are suggested to be involved in inflammation, fibrosis, and disruption of insulin signalling [8,11].

Recent *in vitro* studies have shown that advanced glycation endproducts (AGEs) can alter sphingolipid metabolism [13,14], possibly through the binding with their specific receptor RAGE [15]. AGEs are derived from glycation reactions between sugars or lipids and proteins, resulting in functionally compromised glycated proteins. In addition to the direct impairment of protein function, AGEs can also exert a pro-inflammatory action through the binding to RAGE [16].

We recently demonstrated that AGEs accumulate in target tissues of IR, such as liver, brain, and skeletal muscle of mice exposed to diets rich in either sugars or saturated fats, and in genetically-induced obesity [17–20]. In addition, we also showed that the accumulation of AGEs has been associated to enhanced lipid synthesis, due to deregulation of the lipogenic SCAP/SREBP signalling, resulting in intracellular lipids deposition [17–19,21].

Studies in both animals and humans have demonstrated the direct involvement of AGEs and AGE-RAGE signalling in liver and adipose tissue inflammation and impaired insulin signalling [22–24]. Indeed, the inhibition of AGEs production in obese mice by the anti-glycation agent pyridoxamine reduces intracellular lipid synthesis mediated by sterol regulatory element binding protein 1c (SREBP1c), as well as adiposity and IR [18,25]. Specifically, SREBP1c activation mainly produces palmitic acid which is the substrate for the synthesis of C18-Sph that is rapidly converted to C18–S1P by the sphingosine kinases (SphK) or reacylated to C16-Cer by the ceramide synthases (CerS) [2]. In recent years, the palmitate-derived C16-Cer and C18–S1P have been identified as principal mediators of obesity-related IR [8,26,27].

However, the role of AGEs on sphingolipid metabolism disequilibrium in *in vivo* models of IR has never been explored, so far.

In the present study we thus investigated the presence of hepatic sphingolipid rheostat alterations in rodent models of IR and we evaluated the causal role of AGEs through strategies aimed to prevent AGEs production or to block AGE-RAGE signalling.

2. Materials and methods

2.1. Animals

For the genetically-induced IR model, the liver of non-insulin dependent diabetic C57BLKS-LeptrDb (DbDb) mice (Charles River, Maastricht, the Netherlands), for which physiological parameters and IR was previously reported [22], was here analysed. Mice were cared in compliance with the local ethics committee (Maastricht University) on the use of laboratory animals. At 13 weeks of age DbDb mice and their wild type (WT) counterpart (n = 4–6 per group) were sacrificed, plasma was collected and liver was removed and sectioned for following analysis.

For the diet-induced IR model, we used male C57Bl/6j mice (Charles River Laboratories, Calco, Italy) of 4 weeks of age that were cared in compliance with the European Council directives (No. 86/609/EEC) and with the Principles of Laboratory Animal Care (NIH No. 85-23, revised 1985). The scientific project was approved by the Ethical Committee of the Turin University (permit number: D.M. 94/2012-B). Mice were divided into four groups: a group fed with a standard diet and drinking tapwater (SD group, n = 12), a group fed with a 60% *trans*-fat diet (HFD group, n = 16). Standard diet (Sniff Spezialdiäten GmbH, Soest, Germany) composition was 68% of calories in carbohydrates (36.2% from corn starch, 14.9% from maltodextrin and 11% from sucrose), 13% of calories in fat (soybean oil) and 19% of calories from proteins. HFD diet (Sniff Spezialdiäten GmbH, Soest, Germany) composition was 25% of calories in carbohydrates (12.4% from maltodextrin and 12.6% from sucrose), 59% of calories in fat (5% from soybean, 54% from hydrogenated coconut oil) and 15% of calories from proteins. After four weeks of dietary intervention two subgroups of SD and HFD diet started pyridoxamine supplementation in the drinking water for the remaining eight weeks (SD+P, n = 6; HFD+P, n = 8). All groups received drink and food ad libitum. Body weight and food intake were recorded weekly. Fasting glycemia was measured at the start of the protocol and every 4 weeks by saphenous vein puncture using a glucometer (GlucoGmeter, Menarini Diagnostics). After 10 weeks, mice were sacrificed by cardiac exsanguination. Liver was collected divided into two parts, the first was cryoprotected in Optimal Cutting Temperature compound and the other one frozen in N_2 for cryostatic preparations.

2.2. Oral glucose tolerance test

One day before the diet-induced IR mice were due to be killed, the oral glucose tolerance test (OGTT) was performed after a fasting period of 6 h by administering glucose (2 g/kg) by oral gavage. Once before administration and 15, 30, 60 and 120 min afterward, blood was collected from the saphenous vein, and glucose concentration was measured with a conventional Glucometer (GlucoGmeter; Menarini Diagnostics, Florence, Italy).

2.3. CML incubation on HepG2 cell line

HepG2 cells were cultured in DMEM (1 g/L glucose) supplemented with 20% FCS, 1% penicillin/streptomycin, and 1% non-essential amino acids. CML-modified albumin was prepared by incubating human serum albumin with and without 3 mM glyoxylic acid for 24 h at 37 °C. Albumin incubated without glyoxylic acids served as control-albumin. HepG2 cells were cultured and incubated with 0.5 μM control-albumin and modified CML-albumin during different time periods. In addition, to assess whether CML affects gene expression of sphingolipids enzymes via the RAGE pathway, HepG2 cells were pre-incubated with RAGE antibody (R&D, Minneapolis, USA) (5 μg/ml) to block membranous RAGE, and subsequently incubated with modified CML-albumin.

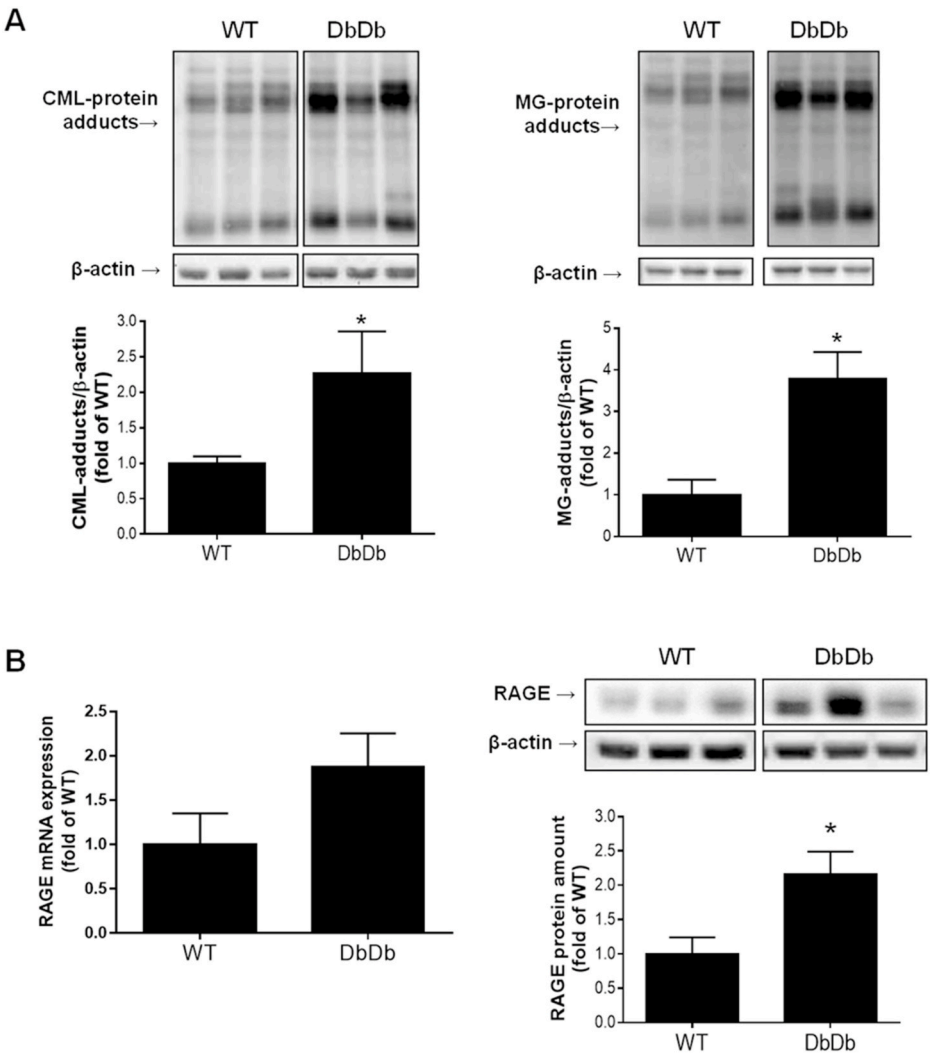

Fig. 1. Accumulation of AGEs and RAGE expression in liver of DbDb mice. Western blotting analysis for CML- and MG-protein adducts in the liver. Histograms of the densitometric analysis normalized for β-actin content and presented as fold-change of WT value (A). Gene and protein expression of RAGE evaluated by RT-PCR and western blotting, respectively, in liver extracts (B). Data are means ± SEM of 4–6 mice per group. Statistical significance: *P<0,05 vs. WT.

2.4. mRNA extracts and PCR analysis

Total RNA was extracted from HepG2 cells and mice livers using TRIzol (Invitrogen, Bleiswijk, the Netherlands) and was reverse transcribed with the iScript cDNA Synthesis Kit (Bio-Rad, Veenendaal, the Netherlands). The expression of target genes was measured quantitatively by real-time PCR using SYBR Green mix (Bioline, London, U.K.). All primer sets used are listed in Supplementary Table 1 mRNA expression levels were normalized to two reference genes (cyclophilin A and β2-microglobulin), and data were analysed with the ΔCT method. Data are expressed as normalized gene expression levels relative to wild-type RAGE+/+ LeptrDb+/+ mice.

2.5. Total, nuclear, and cytosolic protein extracts

Total proteins were obtained from 10% (w/v) mice liver homogenates in RIPA buffer (0.5% Nonidet P-40, 0.5% sodium deoxycholate, 0.1% SDS, 10 mmol/l EDTA, and protease inhibitors). After 40 min of incubation in ice, samples were sonicated and centrifuged at 15,000g at 4 °C for 40 min. Supernatants were collected and stored at −80 °C until use.

Cytosolic and nuclear proteins were extracted from livers homogenized at 10% (wt/vol) in a homogenization buffer containing 20 mM HEPES (pH 7.9), 1 mM $MgCl_2$, 0.5 mM EDTA, 1% Nonidet P-40, 1 mM EGTA, 1 mM DTT, 0.5 mM PMSF, 5 μg/ml aprotinin, 2.5 μg/ml leupeptin and 2 mM $NaVO_3$. Homogenates were centrifuged at 1000g for 5 min at 4 °C. Supernatants were centrifuged at 10,000g at 4 °C for 40 min to isolate the cytosolic fraction. The pelleted nuclei were resuspended in extraction buffer containing 20 mM HEPES (pH 7.9), 1.5 mM $MgCl_2$, 300 mM NaCl, 0.2 mM EDTA, 20% glycerol, 1 mM EGTA, 1 mM DTT, 0.5 mM PMSF, 5 μg/ml aprotinin, 2.5 μg/ml leupeptin and 2 mM $NaVO_3$ and incubated on ice for 30 min for high-salt extraction, followed by centrifugation at 15,000g for 20 min at 4 °C. The resulting supernatants were collected and stored at −80 °C. Protein content was determined using the Bradford assay (Bio-Rad, Hercules, CA, USA).

2.6. UHPLC-MSMS analysis for sphingolipids rheostat intermediates concentrations

The analysis of sphingolipids was performed on liver homogenates using a Nexera (Shimadzu) UHPLC coupled through an ESI source to a QTRAP5500 triple quadrupole analyser (Sciex).

The chromatographic separation was achieved with a kinetex column (1.7 μm, 100 × 2.1 mm, 100 Å, Phenomenex) with 0.1% formic acid in water/acetonitrile 8/2 (eluent A) and 0.1% formic acid in isopropanol/acetonitrile 8/2 (solvent B). Flow rate was set at 400 μL min^{-1}

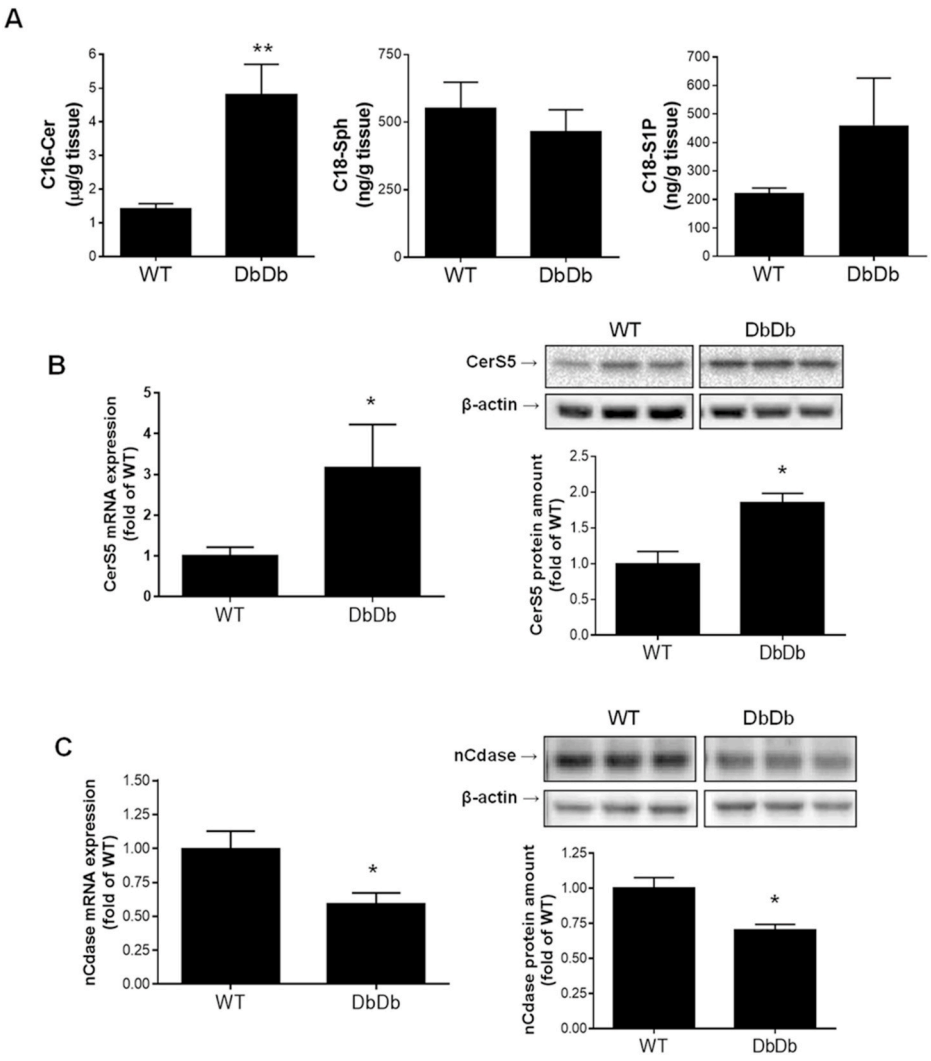

Fig. 2. Sphingolipid rheostat intermediates in the liver of WT and DbDb mice and expression of enzymes responsible for Cer synthesis and degradation. UHPLC-MS/MS analysis of C16-Cer, C18-Sph, and C18–S1P (A). Gene and protein expression of CerS5 (B) and nCdase (C) analysed by RT-PCR and western blotting in liver extracts. Data are means ± SEM of 4–6 mice per group. Statistical significance: *P<0,05; **P<0,01 vs. WT.

and the separation gradient was from 5 to 100% of B in 5 min, followed by column recondition. The LC column effluent was delivered to the ion source, using air as both 1 and 2 gas (40 and 45 arbitrary units respectively). Source ion voltage was 4.5 kV.

The multiple reaction monitoring (MRM) transitions and parameters were: C16-Cer (*m/z*) 538@264 with collision energy (CE) 15%; C18-Sph (*m/z*) 300@282 CE 13%; C18–S1P (*m/z*) 380@264, CE 21%. The lower limit of detection (LLOQ) was 0.50 µg/L for all analytes.

2.7. Western blotting analysis

Through SDS-PAGE we separated equal amounts of proteins and electrotransferred to nitrocellulose membrane (GE-Healthcare Europe, Milano, Italy). After, membranes were probed with primary antibodies, listed in Supplementary Table 2, followed by incubation with appropriated horseradish peroxidase (HRP)-conjugated secondary antibodies (Bio-Rad). The detection of proteins was obtained with Clarity Western ECL substrate (Bio-Rad) and quantified by densitometric analysis software (Quantity-One; Bio-Rad). Results were normalized with respect to densitometric value of mouse anti-β-actin (Santa Cruz Biotechnology) for total and cytosolic extracts and mouse anti-histone H3 (Abcam) for nuclear proteins and then expressed as fold of control mice value.

2.8. Oil Red O staining

Lipid accumulation in the liver was evaluated by Oil Red O staining on 7-µm liver cryostatic sections. Stained tissues were viewed under an Olympus Bx4I microscope (x10, x20 magnification) with an AxioCamMR5 photographic attachment (Zeiss, Gottingen, Germany).

2.9. Stanalysis

The Shapiro-Wilk test was used to assess the normality of the variable distributions. One-way ANOVA followed by Bonferroni's post-hoc test was adopted for comparison among the experimental groups. Data were expressed as mean ± SEM. Statistical tests were performed with GraphPad Prism 7.0 software package (GraphPad Software, San Diego, CA, USA). Threshold for statistical significance was set to P<0.05.

3. Materials

All compounds were purchased from Sigma Chemical, unless otherwise stated.

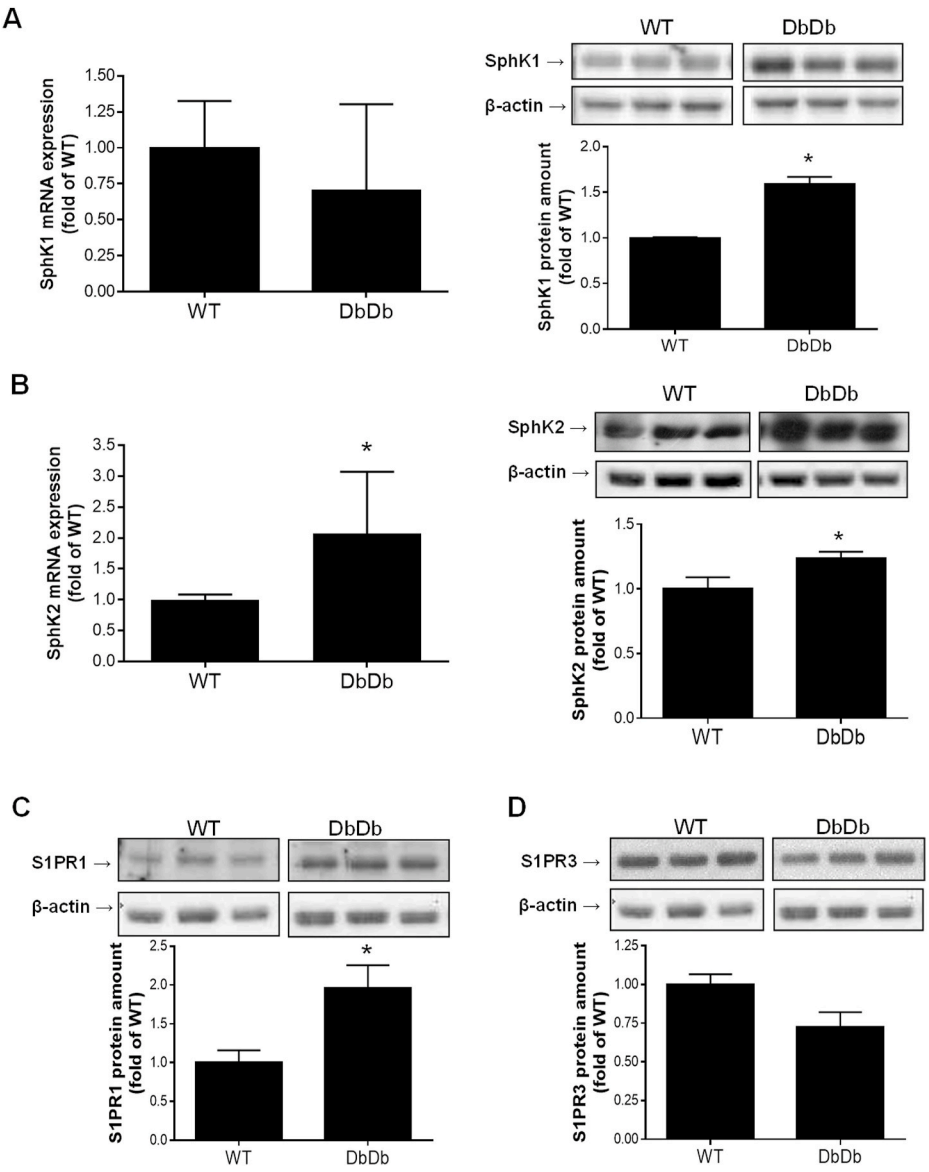

Fig. 3. Expression of enzymes for S1P synthesis and degradation and S1P receptors in the liver of WT and DbDb mice. Gene and protein expression of SphK1 (A) and SphK2 (B) and protein expression of S1PR1 (C) and S1PR3 (D), analysed by RT-PCR and western blotting in liver extracts. Data are means ± SEM of 4–6 mice per group. Statistical significance: *P<0,05 vs. WT.

4. Results

4.1. Genetically-induced insulin resistant mice accumulate AGEs in the liver

To investigate the alterations of sphingolipid intermediates in IR and the role of AGEs, we analysed livers from the DbDb mouse model that was described before [22]. At 13 weeks of age, DbDb mice were obese and insulin resistant as compared to the wild type counterpart [22]. The livers of DbDb mice, compared to WT, showed significantly higher amounts of the AGEs CML- and MG-protein adducts as revealed by western blotting (Fig. 1A). The gene and protein expression of RAGE was markedly increased in the livers of DbDb mice (Fig. 1B).

4.2. Genetically-induced insulin resistant mice have impaired hepatic sphingolipids metabolism

In liver homogenates of DbDb mice, the palmitoyl-derived sphingolipid metabolism intermediate C16-Cer (N-palmitoylsphingosine) was increased and C18–S1P (D-erythro-sphingosine-1-phosphate) tended to be increased ($P = 0.199$), while C18-Sph (D-erythro-sphingosine) was unaltered (Fig. 2A), in comparison to WT mice.

We next analysed the protein expression of the enzymes responsible for the synthesis and degradation of Cer (Fig. 2) and S1P (Fig. 3). In DbDb mice we found markedly increased gene and protein expression of the ceramide synthase 5 (CerS5) (Fig. 2B) and depletion of the mRNA and protein of the neutral ceramidase (nCdase) (Fig. 2C). Although modifications in the gene and protein expression does not necessarily correspond to alterations in enzymatic activity, these changes are in accordance with both the enhanced synthesis and reduced degradation of Cer, respectively.

Moreover, in the liver of DbDb mice we found alterations of the two enzymes responsible for the phosphorylation of Sph to form S1P, with increased protein expression of the sphingosine kinase 1 (SphK1) (Fig. 3A) and increased gene and protein expression of the sphingosine kinase 2 (SphK2) (Fig. 3B), compared to WT.

Since the elevation of S1P is reported to exert extracellular effects through the binding to specific receptors (S1PR1-5) involved in

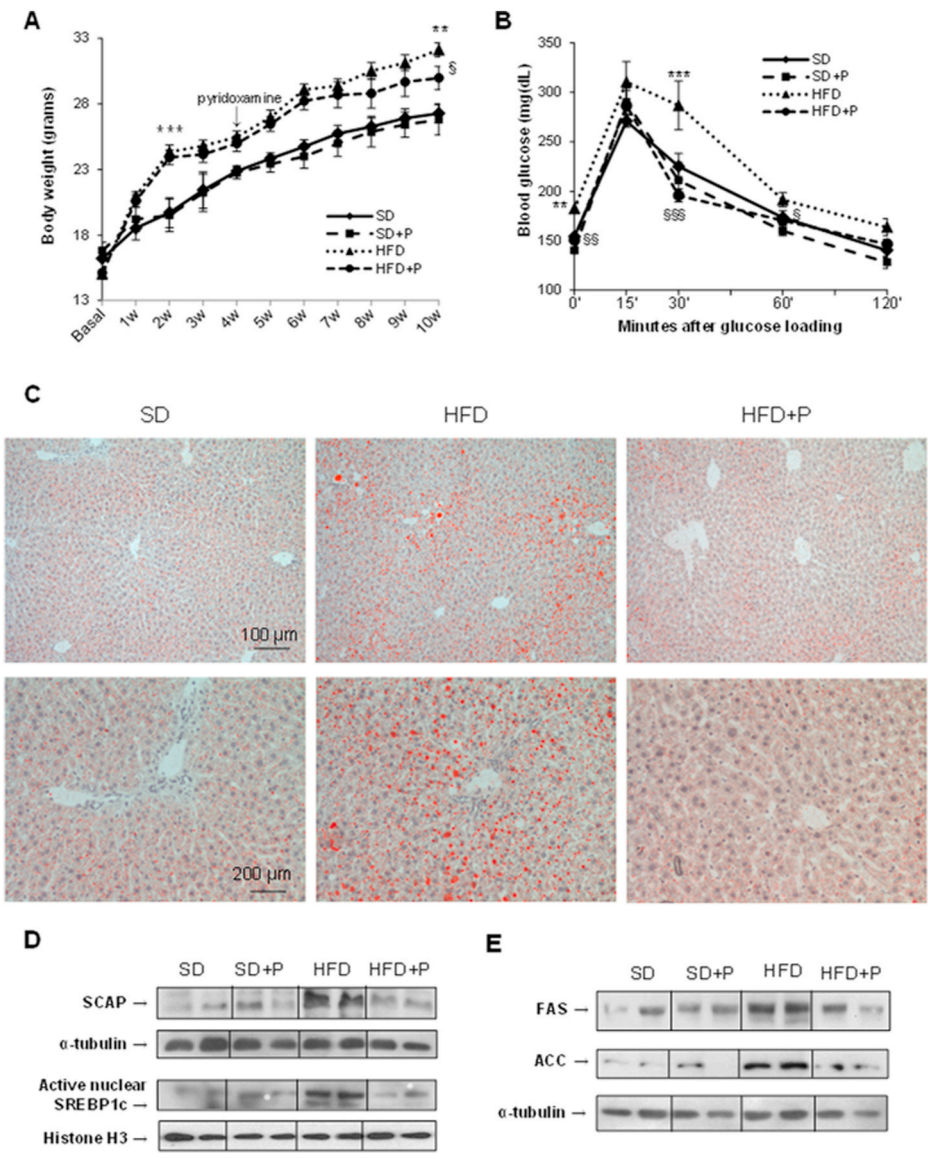

Fig. 4. Weight gain, OGTT, plasma lipid profile, liver lipid accumulation, and liver lipogenesis of HFD mice. Body weight increase during 10 weeks of C57 mice fed a standard diet (SD), a high-trans-fat diet (HFD), supplemented or not with pyridoxamine (150 mg/kg) in the drinking water (HFD + P) starting at the 4 week of diet (A). OGTT performed at the tenth week of dietary manipulation monitoring the blood glucose for 2 h after 2 mg/kg glucose loading by gavage in 6 h fasting mice (B). Plasma (C) and hepatic (D) lipid profile. Oil red O staining in liver sections for the evaluation of neutral lipid deposition (E). Evaluation of the hepatic lipogenesis through analysis of the SCAP/SREBP1c pathway activation (F–H): representative western blotting for the amount of SCAP (F), for the cytosolic and nuclear content of SREBP1c (G), and for the protein levels of FASN and ACC (H). Histograms report the densitometric analysis normalized for α-tubulin or histone H3 content and presented as fold-change of SD value. Data are means ± SEM of 6–8 mice. Statistical significance: **P<0,01; ***P<0,001 vs. SD; §P<0,05; §§P<0,01; §§§P<0,001 vs. HFD.

inflammation and modulation of insulin signalling, we determined the gene expression of some of these specific receptors. We found an upregulation of S1PR1 expression in the liver of DbDb mice compared to WT (Fig. 3C), while the expression of S1PR3 showed a reduction, although this was not statistical significant (Fig. 3D).

4.3. Diet-induced glucose intolerance and lipid accumulation are prevented by pyridoxamine

Since we observed increased hepatic CML levels in the livers of DbDb mice in parallel with alterations of the sphingolipid rheostat, we hypothesized that AGEs could contribute to sphingolipid deregulation. To go deeper into the role of AGEs in sphingolipid rheostat, we used the AGEs inhibitor pyridoxamine, However, since DbDb mice develop very high abnormal circulating levels of leptin [28] which have been proved to interfere with expression and activity of ceramide synthesizing and degrading enzymes [29], we decided to use a HFD-induced model of obesity.

During the ten weeks of dietary manipulation, the HFD mice had a markedly faster weight gain (Fig. 4A) and developed glucose intolerance (Fig. 4B), compared to SD mice. Interestingly, the weight gain of HFD was markedly reduced and glucose intolerance was completely prevented by pyridoxamine supplementation. Similarly, the hepatic steatosis induced by HFD was effectively corrected by pyridoxamine (Fig. 4C).

The lipid accumulation induced by the HFD was likely to be the consequence of the enhanced lipogenesis observed in terms of deregulated activation of the SCAP/SREBP pathway with increased expression of the SREBP cleavage activating protein SCAP (Fig. 4D), increased expression and nuclear translocation of the transcription factor SREBP1c (Fig. 4E), and increased protein levels of its main target genes fatty acid synthase (FASN) and acetyl coenzyme A carboxylase (ACC), as compared to SD mice livers (Fig. 4F). The treatment of HFD fed mice with pyridoxamine normalized SCAP/SREBP lipogenic pathway activation.

Notably, the accumulation of both CML- and MG-glycated proteins (Fig. 5A) and the increased expression of RAGE (Fig. 5B) in the liver of HFD mice were completely abolished by pyridoxamine administration.

4.4. Diet-induced insulin resistant mice have impaired hepatic sphingolipids metabolism which is prevented by pyridoxamine

We next determined whether sphingolipid rheostat was influenced by the HFD. The analysis with UHPLC-MS/MS showed that the Cer/Sph/

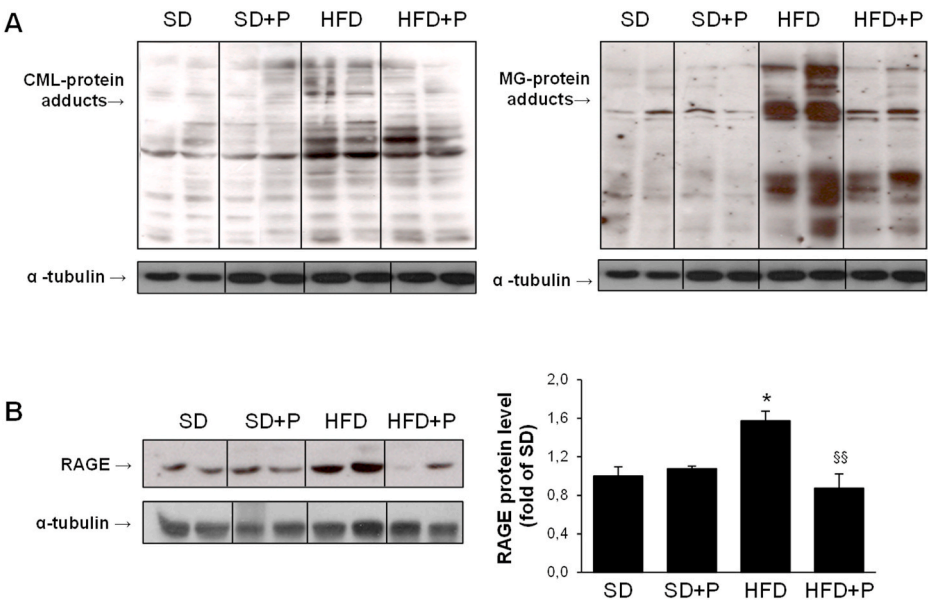

Fig. 5. AGEs accumulation and RAGE expression in liver of HFD mice. Western blotting of CML- and MG-protein adducts (A), and protein expression of RAGE evaluated by RT-PCR and western blotting, respectively (B), in liver extracts of C57BL6/J mice fed a standard diet (SD) or a high-trans-fat diet (HFD), supplemented or not with pyridoxamine (HFD + P). Histograms report the densitometric analysis normalized for α-tubulin content and presented as fold-change of WT value. Data are means ± SEM of 6–8 mice per group. Statistical significance: *P<0,05 vs. WT; §§P<0,01 vs. HFD.

S1P equilibrium was moved towards higher C16-Cer and C18–S1P levels, with concomitant marked reduction of C18-Sph levels (Fig. 6A), similarly to what was observed in the DbDb model. Interestingly, the pyridoxamine administration shifted the equilibrium back to the centre of the balance, by reducing Cer and S1P and inducing an increase in Sph level over the SD values.

In accordance, we found significantly increased protein expression of the CerS5 in HFD, compared to SD-fed mice (Fig. 6B). The pyridoxamine supplementation decreased levels of CerS5. The protein level of the Cer degrading enzyme nCdase in HFD was reduced in comparison to SD mice, accounting for an impaired Cer degradation (Fig. 6C). The pyridoxamine supplementation effectively enhanced the protein expression of nCdase.

On the other side of the balance, the protein level of SphK1 was strongly increased in HFD mice livers in comparison to SD (Fig. 6D), and the pyridoxamine supplementation effectively limited this increase. In addition, the HFD induced a significantly decrease of SphK2 protein levels and the pyridoxamine supplementation reversed the HFD-induced SphK2 downregulation (Fig. 6E).

Moreover, the protein levels of the S1P receptors 1 and 3 were modified by the HFD with increased S1PR1 and reduction of S1PR3 in the liver as compared to SD mice levels (Fig. 6F and G). Pyridoxamine normalized the expression of these S1P receptors in HFD-fed mice.

4.5. Diet-induced insulin resistant mice have impaired hepatic insulin signalling which is prevented by pyridoxamine

Finally, since increased Cer and S1P levels, together with S1P receptors, have been associated to the development of IR, we performed analysis on the phosphorylation status of the main molecules involved in insulin signalling: insulin receptor substrate 1 (IRS) (Fig. 7A), Akt (Fig. 7B), and GSK-3β (Fig. 7C). We found a marked inhibition of insulin signalling in the liver of HFD mice and this effect was attenuated by pyridoxamine.

4.6. CML induces alteration of the sphingolipid enzymes in HepG2 cells through RAGE binding

To confirm the direct involvement of AGEs in sphingolipid metabolism alterations and the possible role of CML-RAGE signalling, we therefore studied the effects of exogenous CML on gene expression of the enzymes involved in regulation of sphingolipids metabolism in HepG2 cells. As shown in Fig. 8, the incubation of HepG2 cells with CML-albumin showed similar alterations as those found in the DbDb and HFD models in the gene expression of CerS5 (Fig. 8A), although not statistical significant (P = 0.484), and nCdase (Fig. 8B). On the other hand, CML-albumin induced increased expression of SphK1 (Fig. 8C), as observed *in vivo*. The blocking of RAGE by a RAGE antibody, effectively reduced the RAGE self-regulated transcription (Fig. 8E) and was able to prevent the CML-induced alterations of CerS5 and of SphK1. Instead, SphK2 expression only showed a slight trend to reduction (P = 0.240) in response to CML treatment that was not detectable when RAGE was blocked (Fig. 8D). In contrast, the downregulation of nCdase induced by CML seemed not to be dependent on RAGE.

5. Discussion

In the present study we have shown that AGEs are involved in the dysregulation of sphingolipid metabolism and insulin sensitivity in the liver. Specifically, in two different murine models of obesity and IR we showed hepatic alterations of the sphingolipid rheostat, with increased levels of Cer and S1P and depletion of Sph. Our *in vivo* results in obese insulin resistant mice showed that the prevention of AGEs accumulation by pyridoxamine in the liver preserve the sphingolipid rheostat, accompanied by an improvement of insulin signalling. Moreover, our *in vitro* experiments in HepG2 cells confirmed that CML influence sphingolipids metabolism through alterations of gene expression of the main enzymes involved in the Cer-Sph-S1P rheostat, similar to those observed in the liver of DbDb and HFD murine models. Blockage of RAGE is only partially effective in the prevention of some of the observed alterations.

Under physiological conditions it is fundamental to control the maintenance of a balanced lipid and glucose metabolism, since in the metabolic syndrome the accumulation of visceral adipose tissue is one of the leading causes, through the promotion of a chronic low-grade inflammatory status, of glucose intolerance and IR. In particular, the sphingolipid rheostat is maintained by the activity of several enzymes and can be perturbed under damaging or pathological conditions such as in obesity, metabolic syndrome, and diabetes. Indeed, in DbDb and HFD-fed mice we found an imbalance of the sphingolipid rheostat as indicated by markedly increased gene and protein expression of the CerS5, accounting for the enhanced specific synthesis of C16-Cer. The increase in Cer synthesis may also be due to reduced degradation by the depletion of the nCdase, as has been shown in INS-1 cells [30,31]. In accordance with our results, increases of CerS5 expression and C16-Cer have been

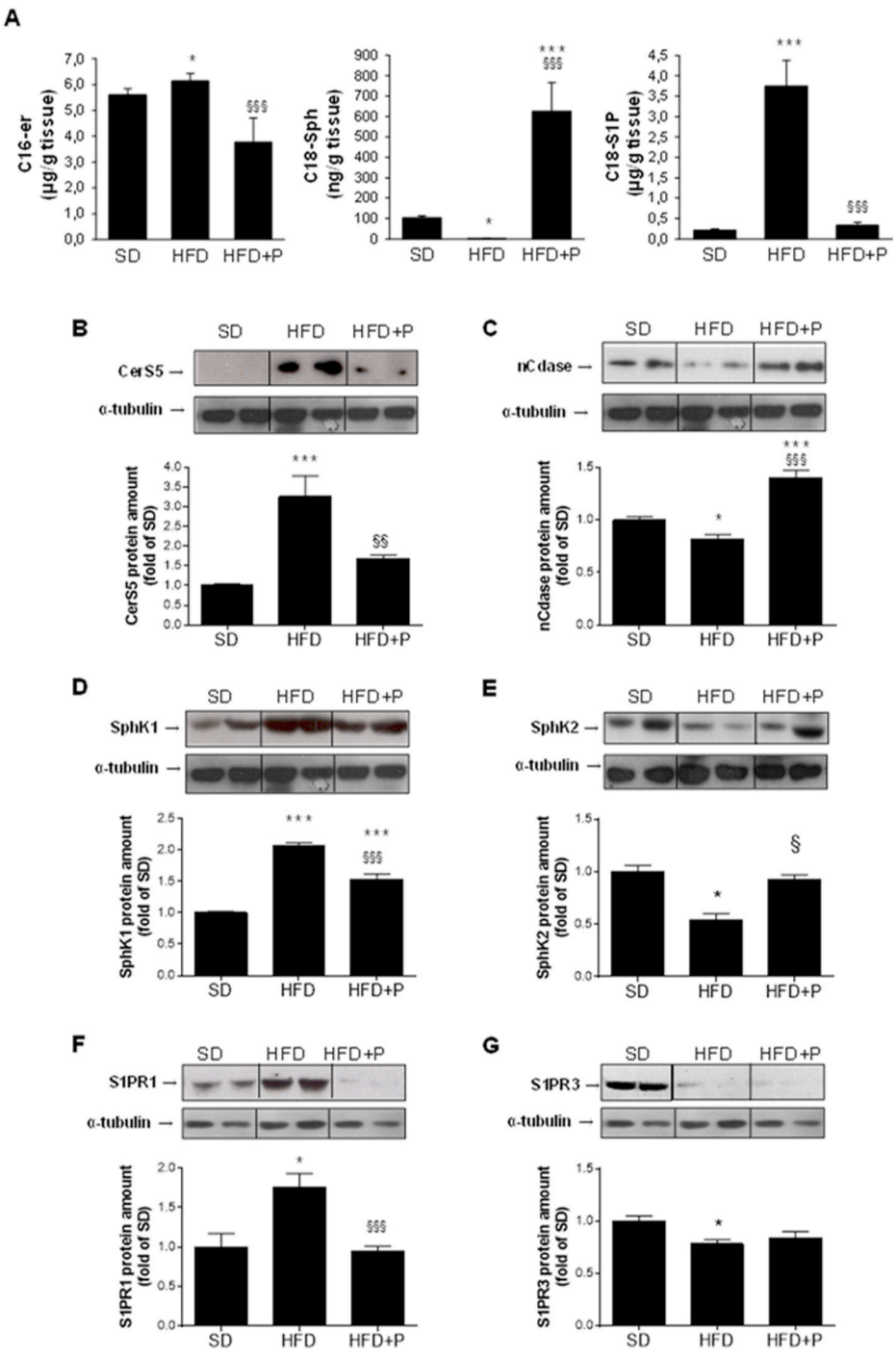

Fig. 6. Sphingolipid metabolism intermediates content and expression of enzymes for ceramide synthesis and degradation and for S1P synthesis, and of S1P receptors in liver of HFD mice. C16-Cer, C18-Sph, and C18– S1P, evaluated by UHPLC-MS/MS in liver homogenates (A). Protein expression evaluated by western blotting analysis for CerS5 (B), nCdase (C), SphK1 (D), SphK2 (E), S1PR1 (F), and S1PR3 (G) in liver extracts. Data are means ± SEM of 6–8 mice. Statistical significance: *P<0,05; ***P<0,001 vs. SD; §P<0,05; §§P<0,01; §§§P<0,001 vs. HFD.

previously observed in white adipose tissue after high-fat diet feeding [32]. Conversely, the genetic inhibition of CerS5 is sufficient to ameliorate obesity and its comorbidities, contributing to maintenance of glucose homeostasis and reduction of white adipose tissue inflammation after a high-fat diet challenge [32].

We found in the HFD model that the prevention of AGEs production by pyridoxamine strongly enhanced Cer degradation, indicating that AGEs alter sphingolipid metabolism. In accordance, direct effect of AGEs on Cer production has been demonstrated in many cultured cell types, including pericytes, fibroblasts, and cardiomiocytes [15,33–35]. Moreover, as assessed in CML-BSA-treated mesangial cells and in glomeruli isolated from STZ-diabetic rats, AGEs exert biphasic effects on both Cdase and SphK1 expression and activity, which are dose- and time-dependent [13].

We showed the involvement of RAGE in increased gene expression of the Cer synthesizing enzymes, while no contribution of RAGE seems to be involved in altered expression of the Cer degrading enzymes. The RAGE-dependent increase of Cer production is in line with data in RAGE overexpressing mice [15].

In addition to altered expression of the Cer synthesizing and degrading enzymes in the liver of both DbDb and HFD mice, we found also increased expression of the SphK1. The protein level of the SphK2 was increased in the DbDB, but decreased in the liver of the HFD model and in CML-treated HepG2 cells. Most importantly, altered expression of SphK1 and SphK2 was effectively prevented by pyridoxamine. In line, increased expression and activity of SphK1 were previously detected in

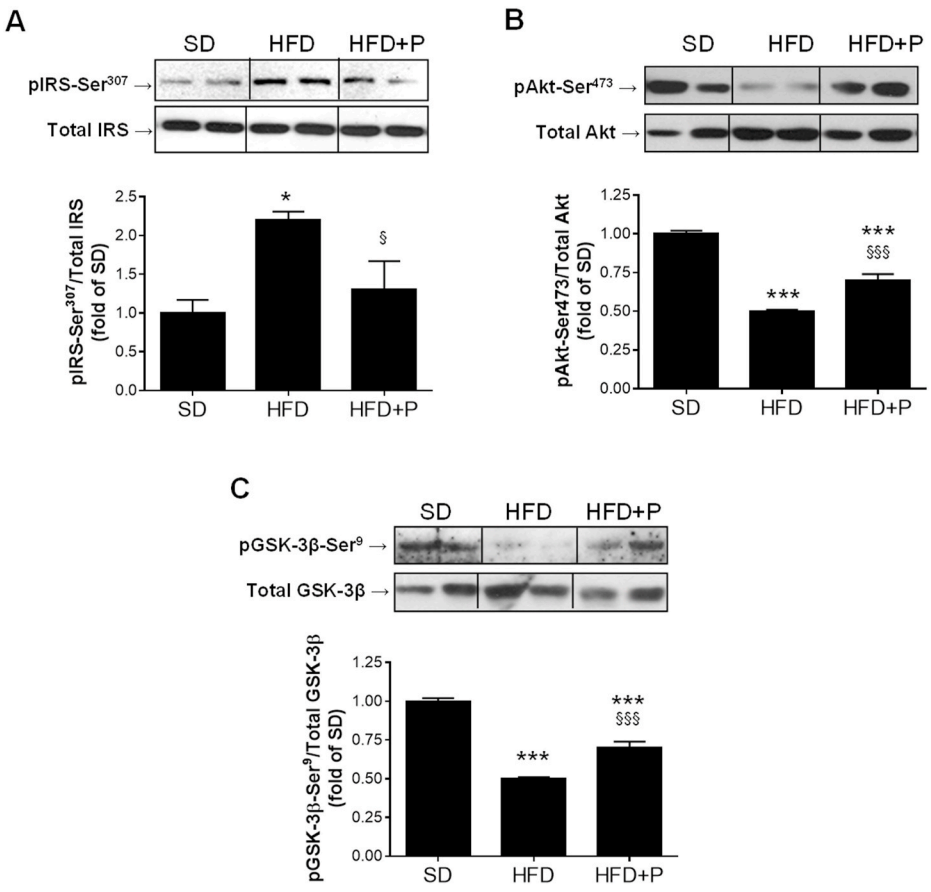

Fig. 7. Insulin signalling in liver of HFD mice. Western blotting of the phosphorylated and total forms of IRS (A), Akt (B), and GSK-3β (C) in liver extracts of C57 mice fed a standard diet (SD), a high-trans-fat diet (HFD), supplemented or not with pyridoxamine. Data are means ± SEM of 6–8 mice. Statistical significance: *P<0,05; ***P<0,001 vs. SD; §P<0,05; §§§P<0,001 vs. HFD.

the kidney of DbDb mice associated to fibrosis, and the treatment of cultured mesangial cells with AGEs has been able to induce SphK1 expression and consequent increase of S1P levels, leading to the onset of an inflammatory response. In accordance, the treatment with polydatin, a natural antioxidant compound with anti-glycation properties, showed a reduction of SphK1 expression and profibrotic and proinflammatory signalling in both kidney and mesangial cells [14].

The direct interaction between AGEs and SphK1 activity and their role in the fibrotic process has been demonstrated in a recent elegant work by Chen et al. [36] in which they showed that the treatment of glomerular mesangial cells with AGEs-BSA induces SphK1 expression and activity and increase S1P levels. The effect of AGEs is, at least in part, mediated by AGE-RAGE binding [36]. Furthermore, in an animal model of type 1 diabetes, the anti-glycation compound aminoguanidine prevented the overexpression of SphK1 and the production of S1P in the kidney, accompanied by the amelioration of renal injury and fibrosis. The proposed mechanism was a decrease of SphK1 ubiquitination and degradation, thus leading to a prolonged activity [36]. Noteworthy, we reported significant alterations in the expression of enzymes involved in sphingolipid rheostat that may not imply altered enzymatic activity. However, the correspondent impairment of the sphingolipid intermediates concentrations in the liver suggests that the observed modifications in enzyme protein levels are also paralleled by altered activity, as confirmed by many of the abovementioned literature data reporting accordance between modifications in expression and enzymatic activity of the considered enzymes.

The induced SphK1 expression leads to the exit of newly synthesized S1P in the extracellular space resulting in induction of the proinflammatory NFkB signalling with activation of TNF-alpha and MCP-1. In a rat model of fructose diet-induced hepatosteatosis increased expressions of S1PR1 and S1PR3 have been detected in the liver associated to enhanced NFkB activation and IL-6 and TNF-alpha levels [11]. In particular, previous works demonstrated that the S1P receptor-1 (S1PR1) was responsible for the inflammatory response activation on HepG2 cells [11,37].

We found and increased expression of S1PR1 in the liver of DbDb mice and HFD mice, while S1PR3 was reduced. This is in accordance with studies demonstrating different mechanisms of regulation and action of these two S1P receptors depending on specific metabolic conditions [38]. Of interest, the reduction of AGEs accumulation by pyridoxamine in the liver of HFD mice was associated with a normalisation of the expression of both the analysed S1P receptors.

The here observed ability of pyridoxamine to reduce lipid synthesis and preserve the expression levels of the sphingolipids metabolism enzymes finally results in the prevention of liver lipotoxicity and insulin signalling impairment.

6. Conclusions

Taken together, the results of the current study show that the accumulation of AGEs in the liver in different models of IR influences the lipid metabolism and in particular the sphingolipid rheostat. The mechanisms of AGEs in the imbalance of the rheostat are likely to be due to both the direct effect of AGEs and, although only in part, to the activation of RAGE signalling leading to alterations of the expression of the enzymes involved in the maintenance of the sphingolipid metabolism equilibrium. The precise link between AGEs and/or AGE-RAGE signalling and the transcriptional effects on the genes encoding for the

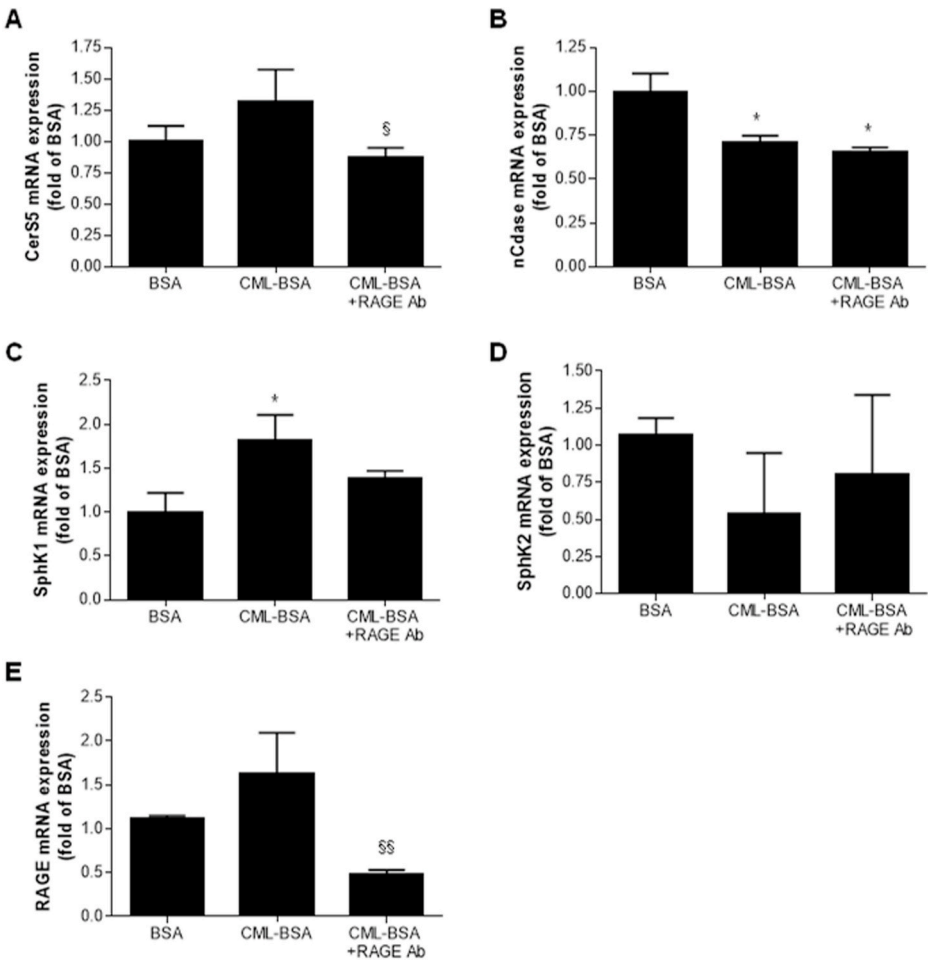

Fig. 8. Expression of sphingolipids metabolism enzymes and RAGE in CML-treated HepG2 cells. Gene expression of CerS5 (A), nCdase (B), SphK1 (C), SphK2 (D), and RAGE (E) analysed by RT-PCR in mRNA extracts of HepG2 cells incubated with control-albumin (BSA), modified CML-albumin (CML-BSA), and modified CML-albumin with pre-incubation with RAGE antibody (CML-BSA + RAGE Ab). Data are means ± SEM of three separate experiments. Statistical significance: *P<0,05 vs. BSA; §P<0,05; §§P<0,01 vs. CML-BSA.

sphingolipid rheostat enzymes still needs to be investigated.

In summary, the AGEs production is a link between alterations in sphingolipid metabolism and the IR development in liver tissue. The AGEs-sphingolipid rheostat axis may be a novel therapeutic target and preventive strategy for lipid and glucose metabolism disturbances.

Funding

This research was funded by the University of Turin (grant ID: Ricerca Locale Ex-60%). International mobility of Dr. Mastrocola to the Maastricht University was funded by an EMBO short-term fellowship. Authors are responsible for the contents of the present work.

Authors contribution

Conceptualization, CGS and RM; methodology, FDB, ASC, KHG, DC; validation, MA, CM and MC; formal analysis, FDB, ASC, KHG, DC; investigation, FDB, ASC, KHG, DC; resources, CGS and RM; data curation, KW, CGS and RM; writing-original draft preparation, CGS and RM; writing—review and editing, KW, CM and MC; supervision, CGS and RM; funding acquisition, CGS and RM.

All authors have read and agreed to the published version of the manuscript.

Declaration of competing interest

The authors declare no conflict of interest.

Acknowledgments

Authors acknowledge Margee Teunissen for her precious technical support.

Appendix A. Supplementary data

Supplementary data to this article can be found online at https://doi.org/10.1016/j.freeradbiomed.2021.04.028.

References

[1] B. Mittendorfer, Origins of metabolic complications in obesity: adipose tissue and free fatty acid trafficking, Curr. Opin. Clin. Nutr. Metab. Care 14 (2011) 535–541, https://doi.org/10.1097/MCO.0b013e32834ad8b6.

[2] S. Choi, A.J. Snider, Sphingolipids in high fat diet and obesity-related diseases, Mediat. Inflamm. 2015 (2015), https://doi.org/10.1155/2015/520618.

[3] C. Mao, L.M. Obeid, Ceramidases: regulators of cellular responses mediated by ceramide, sphingosine, and sphingosine-1-phosphate, Biochim. Biophys. Acta Mol. Cell Biol. Lipids 1781 (2008) 424–434, https://doi.org/10.1016/j.bbalip.2008.06.002.

[4] J.M. Haus, S.R. Kashyap, T. Kasumov, R. Zhang, K.R. Kelly, R.A. Defronzo, J. P. Kirwan, Plasma ceramides are elevated in obese subjects with type 2 diabetes and correlate with the severity of insulin resistance, Diabetes 58 (2009) 337–343, https://doi.org/10.2337/db08-1228.

[5] X. Tong, H. Peng, D. Liu, L. Ji, C. Niu, J. Ren, B. Pan, J. Hu, L. Zheng, Y. Huang, High-density lipoprotein of patients with Type 2 Diabetes Mellitus upregulates cyclooxgenase-2 expression and prostacyclin I-2 release in endothelial cells: relationship with HDL-associated sphingosine-1-phosphate, Cardiovasc. Diabetol. 12 (2013) 1–9, https://doi.org/10.1186/1475-2840-12-27.

[6] S. Ito Shioria, Soichiroa Iwaki, Keikoa Koike, Yuichiroa Yuda, Ayakoa Nagasaki, Ryunosukeb Ohkawa, Yutakab Yatomi, Tomooc Furumoto, Hiroyukic Tsutsui, Burton E.d Sobel, Fujii, Increased plasma sphingosine-1-phosphate in obese individuals and its capacity to increase the expression of plasminogen activator

inhibitor-1 in adipocytes, Coron. Artery Dis. 24 (2013) 642–650, https://doi.org/10.1097/MCA.0000000000000033.
[7] Y. Ilan, Compounds of the sphingomyelin-ceramide-glycosphingolipid pathways as secondary messenger molecules: new targets for novel therapies for fatty liver disease and insulin resistance, Am. J. Physiol. Gastrointest. Liver Physiol. 310 (2016) G1102–G1117, https://doi.org/10.1152/ajpgi.00095.2016.
[8] S. Fayyaz, J. Henkel, L. Japtok, S. Krämer, G. Damm, D. Seehofer, G.P. Püschel, B. Kleuser, Involvement of sphingosine 1-phosphate in palmitate-induced insulin resistance of hepatocytes via the S1P2 receptor subtype, Diabetologia 57 (2014) 373–382, https://doi.org/10.1007/s00125-013-3123-6.
[9] K. Kurek, B. Łukaszuk, D.M. Piotrowska, P. Wiesiołek, A.M. Chabowska, M. Zendzian-Piotrowska, Metabolism, physiological role, and clinical implications of sphingolipids in gastrointestinal tract, BioMed Res. Int. 2013 (2013), https://doi.org/10.1155/2013/908907.
[10] W.J. Park, J.H. Song, G.T. Kim, T.S. Park, Ceramide and sphingosine 1-phosphate in liver diseases, Mol. Cells. 43 (2020) 419–430, https://doi.org/10.14348/molcells.2020.0054.
[11] X. Wang, D.M. Zhang, T.T. Gu, X.Q. Ding, C.Y. Fan, Q. Zhu, Y.W. Shi, Y. Hong, L. D. Kong, Morin reduces hepatic inflammation-associated lipid accumulation in high fructose-fed rats via inhibiting sphingosine kinase 1/sphingosine 1-phosphate signaling pathway, Biochem. Pharmacol. 86 (2013) 1791–1804, https://doi.org/10.1016/j.bcp.2013.10.005.
[12] J.R. Ussher, T.R. Koves, V.J.J. Cadete, L. Zhang, J.S. Jaswal, S.J. Swyrd, D. G. Lopaschuk, S.D. Proctor, W. Keung, D.M. Muoio, G.D. Lopaschuk, Inhibition of de novo ceramide synthesis reverses diet-induced insulin resistance and enhances whole-body oxygen consumption, Diabetes 59 (2010) 2453–2464, https://doi.org/10.2337/db09-1293.
[13] K. Geoffroy, N. Wiernsperger, M. Lagarde, S. El Bawab, Bimodal effect of advanced glycation end products on mesangial cell proliferation is mediated by neutral ceramidase regulation and endogenous sphingolipids, J. Biol. Chem. 279 (2004) 34343–34352, https://doi.org/10.1074/jbc.M403273200.
[14] C. Chen, K. Huang, J. Hao, J. Huang, Z. Yang, F. Xiong, P. Liu, H. Huang, Polydatin attenuates AGEs-induced upregulation of fibronectin and ICAM-1 in rat glomerular mesangial cells and db/db diabetic mice kidneys by inhibiting the activation of the SphK1-S1P signaling pathway, Mol. Cell. Endocrinol. 427 (2016) 45–56, https://doi.org/10.1016/j.mce.2016.03.003.
[15] M.B. Nelson, A.C. Swensen, D.R. Winden, J.S. Bodine, B.T. Bikman, P.R. Reynolds, Cardiomyocyte mitochondrial respiration is reduced by receptor for advanced glycation end-product signaling in a ceramide-dependent manner, Am. J. Physiol. Heart Circ. Physiol. 309 (2015) H63–H69, https://doi.org/10.1152/ajpheart.00043.2015.
[16] L. Engelen, C.D.A. Stehouwer, C.G. Schalkwijk, Current therapeutic interventions in the glycation pathway: evidence from clinical studies, Diabetes Obes. Metabol. 15 (2013) 677–689, https://doi.org/10.1111/dom.12058.
[17] R. Mastrocola, M. Collino, M. Rogazzo, C. Medana, D. Nigro, G. Boccuzzi, M. Aragno, Advanced glycation end products promote hepatosteatosis by interfering with SCAP-SREBP pathway in fructose-drinking mice, Am. J. Physiol. Gastrointest. Liver Physiol. 305 (2013) G398–G407, https://doi.org/10.1152/ajpgi.00450.2012.
[18] R. Mastrocola, D. Nigro, F. Chiazza, C. Medana, F. Dal Bello, G. Boccuzzi, M. Collino, M. Aragno, Fructose-derived advanced glycation end-products drive lipogenesis and skeletal muscle reprogramming via SREBP-1c dysregulation in mice, Free Radic. Biol. Med. 91 (2016), https://doi.org/10.1016/j.freeradbiomed.2015.12.022.
[19] R. Mastrocola, M. Collino, D. Nigro, F. Chiazza, G. D'Antona, M. Aragno, M. A. Minetto, Accumulation of advanced glycation end-products and activation of the SCAP/SREBP lipogenetic pathway occur in diet-induced obese mouse skeletal muscle, PloS One 10 (2015), https://doi.org/10.1371/journal.pone.0119587.
[20] R. Mastrocola, D. Nigro, A.S. Cento, F. Chiazza, M. Collino, M. Aragno, High-fructose intake as risk factor for neurodegeneration: key role for carboxy methyllysine accumulation in mice hippocampal neurons, Neurobiol. Dis. 89 (2016), https://doi.org/10.1016/j.nbd.2016.02.005.
[21] M. Bijnen, M.M.J. Van Greevenbroek, C.J.H. Van Der Kallen, J.L. Scheijen, M.P. H. Van De Waarenburg, C.D.A. Stehouwer, K. Wouters, C.G. Schalkwijk, Hepatic fat content and liver enzymes are associated with circulating free and protein-bound advanced glycation end products, which are associated with low-grade inflammation: the CODAM study, J. Diabetes Res. 2019 (2019), https://doi.org/10.1155/2019/6289831.
[22] K.H.J. Gaens, G.H. Goossens, P.M. Niessen, M.M. van Greevenbroek, C.J.H. van der Kallen, H.W. Niessen, S.S. Rensen, W.A. Buurman, J.W.M. Greve, E.E. Blaak, M. A. van Zandvoort, A. Bierhaus, C.D.A. Stehouwer, C.G. Schalkwijk, Nε-(carboxymethyl)lysine-receptor for advanced glycation end product axis is a key modulator of obesity-induced dysregulation of adipokine expression and insulin resistance, Arterioscler. Thromb. Vasc. Biol. 34 (2014) 1199–1208, https://doi.org/10.1161/ATVBAHA.113.302281.
[23] K.H.J. Gaens, P.M.G. Niessen, S.S. Rensen, W.A. Buurman, J.W.M. Greve, A. Driessen, M.G.M. Wolfs, M.H. Hofker, J.G. Bloemen, C.H. Dejong, C.D. A. Stehouwer, C.G. Schalkwijk, Endogenous formation of Nε-(carboxymethyl) lysine is increased in fatty livers and induces inflammatory markers in an in vitro model of hepatic steatosis, J. Hepatol. 56 (2012) 647–655, https://doi.org/10.1016/j.jhep.2011.07.028.
[24] K.H.J. Gaens, I. Ferreira, M.P.H. Van De Waarenburg, M.M. Van Greevenbroek, C.J. H. Van Der Kallen, J.M. Dekker, G. Nijpels, S.S. Rensen, C.D.A. Stehouwer, C. G. Schalkwijk, Protein-Bound plasma nε-(carboxymethyl)lysine is inversely associated with central obesity and inflammation and significantly explain a part of the central obesity-related increase in inflammation: the hoorn and CODAM studies, Arterioscler. Thromb. Vasc. Biol. 35 (2015) 2707–2713, https://doi.org/10.1161/ATVBAHA.115.306106.
[25] D.E. Maessen, O. Brouwers, K.H. Gaens, K. Wouters, J.P. Cleutjens, B.J. Janssen, T. Miyata, C.D. Stehouwer, C.G. Schalkwijk, Delayed intervention with pyridoxamine improves metabolic function and prevents adipose tissue inflammation and insulin resistance in high-fat diet-induced obese mice, Diabetes 65 (2016) 956–966, https://doi.org/10.2337/db15-1390.
[26] S.M. Turpin, H.T. Nicholls, D.M. Willmes, A. Mourier, S. Brodesser, C. M. Wunderlich, J. Mauer, E. Xu, P. Hammerschmidt, H.S. Brönneke, A. Trifunovic, G. Losasso, F.T. Wunderlich, J.W. Kornfeld, M. Blüher, M. Krönke, J.C. Brüning, Obesity-induced CerS6-dependent C16:0 ceramide production promotes weight gain and glucose intolerance, Cell Metabol. 20 (2014) 678–686, https://doi.org/10.1016/j.cmet.2014.08.002.
[27] S. Raichur, S.T. Wang, P.W. Chan, Y. Li, J. Ching, B. Chaurasia, S. Dogra, M. K. Öhman, K. Takeda, S. Sugii, Y. Pewzner-Jung, A.H. Futerman, S.A. Summers, CerS2 haploinsufficiency inhibits β-oxidation and confers susceptibility to diet-induced steatohepatitis and insulin resistance, Cell Metabol. 20 (2014) 687–695, https://doi.org/10.1016/j.cmet.2014.09.015.
[28] B. Wang, P. Chandrasekera, J. Pippin, Leptin- and leptin receptor-deficient rodent models: relevance for human type 2 diabetes, Curr. Diabetes Rev. 10 (2014) 131–145, https://doi.org/10.2174/1573399810666140508121012.
[29] E. Bonzón-Kulichenko, D. Schwudke, N. Gallardo, E. Moltó, T. Fernández-Agulló, A. Shevchenko, A. Andrés, Central leptin regulates total ceramide content and sterol regulatory element binding protein-1C proteolytic maturation in rat white adipose tissue, Endocrinology 150 (2009) 169–178, https://doi.org/10.1210/en.2008-0505.
[30] F. Luo, Y. Feng, H. Ma, C. Liu, G. Chen, X. Wei, X. Mao, X. Li, Y. Xu, S. Tang, H. Wen, J. Jin, Q. Zhu, Neutral ceramidase activity inhibition is involved in palmitate-induced apoptosis in INS-1 cells, Endocr. J. 64 (2017) 767–776, https://doi.org/10.1507/endocrj.EJ16-0512.
[31] Q. Zhu, R. Zhu, J. Jin, Neutral ceramidase-enriched exosomes prevent palmitic acid-induced insulin resistance in H4IIEC3 hepatocytes, FEBS Open Bio 6 (2016) 1078–1084, https://doi.org/10.1002/2211-5463.12125.
[32] D. Gosejacob, P.S. Jäger, K. Vom Dorp, M. Frejno, A.C. Carstensen, M. Köhnke, J. Degen, P. Dörmann, M. Hoch, Ceramide synthase 5 is essential to maintain C16: 0-Ceramide pools and contributes to the development of diet-induced obesity, J. Biol. Chem. 291 (2016) 6989–7003, https://doi.org/10.1074/jbc.M115.691212.
[33] S. Patschan, J. Chen, A. Polotskaia, N. Mendelev, J. Cheng, D. Patschan, M. S. Goligorsky, Lipid mediators of autophagy in stress-induced premature senescence of endothelial cells, Am. J. Physiol. Heart Circ. Physiol. 294 (2008) 1119–1129, https://doi.org/10.1152/ajpheart.00713.2007.
[34] U. Denis, M. Lecomte, C. Paget, D. Ruggiero, N. Wiernsperger, M. Lagarde, Advanced glycation end-products induce apoptosis of bovine retinal pericytes in culture: involvement of diacylglycerol/ceramide production and oxidative stress induction, Free Radic. Biol. Med. 33 (2002) 236–247, https://doi.org/10.1016/S0891-5849(02)00879-1.
[35] M. Alikhani, C.M. MacLellan, M. Raptis, S. Vora, P.C. Trackman, D.T. Graves, Advanced glycation end products induce apoptosis in fibroblasts through activation of ROS, MAP kinases, and the FOXO1 transcription factor, Am. J. Physiol. Cell Physiol. 292 (2007) 850–856, https://doi.org/10.1152/ajpcell.00356.2006.
[36] C. Chen, W. Gong, C. Li, F. Xiong, S. Wang, J. Huang, Y. Wang, Z. Chen, Q. Chen, P. Liu, T. Lan, H. Huang, Sphingosine kinase 1 mediates AGEs-induced fibronectin upregulation in diabetic nephropathy, Oncotarget 8 (2017) 78660–78676, https://doi.org/10.18632/oncotarget.20205.
[37] T. Geng, A. Sutter, M.D. Harland, B.A. Law, J.S. Ross, D. Lewin, A. Palanisamy, S. B. Russo, K.D. Chavin, L.A. Cowart, SphK1 mediates hepatic inflammation in a mouse model of NASH induced by high saturated fat feeding and initiates proinflammatory signaling in hepatocytes, J. Lipid Res. 56 (2015) 2359–2371, https://doi.org/10.1194/jlr.M063511.
[38] J. Guitton, C.L. Bandet, M.L. Mariko, S. Tan-Chen, O. Bourron, Y. Benomar, E. Hajduch, H. Le Stunff, Sphingosine-1-Phosphate metabolism in the regulation of obesity/type 2 diabetes, Cells 9 (2020) 1–19, https://doi.org/10.3390/cells9071682.